SiliconPV 2023, 13th International Conference on Crystalline Silicon Photovoltaics
Silicon Material and Defect Engineering
https://doi.org/10.52825/siliconpv.v1i.840

Published: 22 Feb. 2024

Reducing Time and Costs of FT-IR Studies of the Effect of SiN_x, Dopants, and Emitter on Hydrogen Species in Si Wafers and Solar Cell Structures

Nicole Aßmann[1][https://orcid.org/0000-0001-8036-416X], Rune Søndenå[2][https://orcid.org/0000-0001-7533-3676], Benjamin Hammann[3,4][https://orcid.org/0000-0002-3530-4181], Wolfram Kwapil[3,4][https://orcid.org/0000-0001-8489-1805], and Eduard Monakhov[1][https://orcid.org/0000-0002-7015-3358]

[1] Centre for Materials Science and Nanotechnology, University of Oslo, N-0318 Oslo, Norway

[2] Institute for Energy Technology, N-2007, Kjeller, Norway

[3] Fraunhofer Institute for Solar Energy Systems ISE, 79110 Freiburg, Germany

[4] University of Freiburg, Department of Sustainable Systems Engineering (INATECH), 79110 Freiburg, Germany

Abstract. Accurately measuring the hydrogen content in silicon (Si) solar cells is essential due to its connection to surface degradation and light and elevated temperature induced degradation (LeTID). Fourier Transform-Infrared (FT-IR) spectroscopy provides a quantitative technique for determining the content of various hydrogen species in Si wafers that have undergone various process steps. In this study, we examine both the effect of a silicon nitride (SiN_x:H) layer during FT-IR spectroscopic measurements on hydrogen species, as well as the impact of an emitter present during firing on the amount of hydrogen introduced into Si wafers. We find that the presence of SiN_x:H during measurements has negligible effects on the measured hydrogen species, potentially simplifying the preparation steps for FT-IR. For the emitter investigation we analyze boron (B)- and gallium (Ga)-doped p-type wafers to detect H-B, H-Ga, O_i-H_2, and H_2. We observe that hydrogen species initially present in B- and Ga-doped Si wafers differ significantly. Only H-Ga is detected in Ga-doped wafers, while H-B, O_i-H_2, and H_2 signals are measured in B-doped wafers. Moreover, we cannot confirm an increased release of H through the emitter into the bulk during the firing process. Finally, we conduct measurements at different temperatures and confirm that cryogenic temperatures are more effective for detecting H-B and H_2 with concentrations in the 10^{14} cm^{-3} range. Nevertheless, useful spectra can still be obtained at liquid nitrogen (N_2) temperatures.

Keywords: FT-IR Spectroscopy, Hydrogen Detection, Photovoltaics, Silicon

1. Introduction

Hydrogen (H) is an important contributor in silicon (Si) solar cells performance. It serves for bulk defect passivation as well as surface passivation [1], [2], [3]. In contrary, H has been identified as responsible species to cause light and elevated temperature induced degradation (LeTID) (e.g., in [4], [5], [6]), a charge carrier lifetime reducing degradation phenomenon, reported for the first time by Ramspeck et al. in 2012 [7].

Tied to hydrogen in Si solar cells are two commonly used layers in p-type Si-based solar cells: the hydrogen-rich silicon nitride (SiN_x:H) layer and the phosphorus doped emitter. During the contact firing process step in production, SiN_x:H releases hydrogen into the bulk and serves as the primary source of H. Furthermore, current understanding suggests that the presence of

an emitter during firing also increases the hydrogen content: Chen et al. [8] have reported an increased LeTID when highly doped layers were present during firing for n-type Czochralski-grown (Cz) Si. They attribute this phenomenon to the emitter acting as a barrier for out-diffusion of hydrogen.

The detection of hydrogen-related species in commercial silicon wafers is a challenging task due to their low concentrations, which are typically at around 10^{15} cm^{-3} and lower. Wolny et al. [9] presented a technique to measure interstitial oxygen (O_i) in Si wafers by FT-IR spectroscopy: Instead of the conventional orientation of the IR beam normal to the bulk material, they let the IR beam transmit longitudinally through a stack of two to four Si wafers with a pathlength of 2 mm. Similarly, we have proposed that an increased pathlength of around 10 mm enables detection of low concentration H related signals [10]. This advanced characterization method is capable of distinguishing between various hydrogen-containing species based on their localized vibrational modes (LVMs) as well as quantifying their concentration. Its feasibility has been demonstrated for instance in [11] and [12].

Jonak-Auer et al. [13] previously proposed a FT-IR spectroscopy-based method for measuring the hydrogen content of SiNx:H films on Si material. This indicates that the presence of the layer may interfere with the measurement of the H content of the bulk. Therefore, to ensure reliable results, the SiN_x:H layer is typically removed prior to measurements.

FT-IR spectroscopy at cryogenic temperatures provides high sensitivities with sharp signals and a detection limit of ~10^{13} cm^{-3}. However, it is time- and energy-intensive, which may be considered a drawback. In contrast, room temperature measurements are simpler but have a higher detection limit of $2 \cdot 10^{14}$ cm^{-3} [14] rendering them less competitive. Investigating several temperatures between these extremes can lead to a compromise that balances sensitivity and practicality.

In this study we investigate (i) the influence of SiN_x:H layers present during FT-IR measurements, (ii) the hydrogen content released through firing of the emitter layer, and (iii) the influence of different measurement temperatures on the resulting spectra.

2. Experimental Details

2.1. Sample Preparation

In this study p-type Si wafers with a bulk resistivity of 1 Ωcm were used. They differ by the process steps they went through for investigating (a) the influence of SiN_x:H layers present during measurement on the results and (b) the effect of an emitter presence during firing on the hydrogen content of the samples. An overview is given in Fig. 1: (a) Boron-doped float zone (FZ) wafers with a thickness of 250 µm, and (b) Czochralski-grown (Cz) wafers with a thickness of 180 µm, B- and Ga-doped were used.

For (a), see Fig. 1 (a), the wafers received an RCA cleaning sequence and hydrofluoric acid (HF) dip to remove thermal oxides, followed by an oxidation step at 1050 °C for 60 min. The wafers were then passivated with a 10 nm thick Al_2O_3 (deposited with atomic layer deposition at around 230 °C) and a 100 nm thick SiN_x:H (deposited by plasma-enhanced chemical vapor deposition (PECVD)) at around 400 °C. The subsequent firing step had a measured peak temperature of around 800 °C in a belt furnace. Eventually the Al_2O_3 and SiN_x:H layers were removed for one subset (FZB1) by dipping them into 10 % hydrofluoric acid (HF) for about 15 min. The other set kept the SiN_x:H layer (FZB2).

For (b), see Fig. 1 (b), all wafers were surface damage etched in an HNA solution (hydrofluoric, nitric, and acetic acids). A subsequent two-sided emitter in-diffusion in a tube furnace ($POCl_3$, ca. 70 Ω/sq, 833 °C) was performed for two samples (CzB1 and CzGa1), whereas two samples (CzB2 and CzGa2) remained non-diffused.

A 76 nm thick SiN_x:H layer was then deposited by PECVD at around 400 °C, followed by a simulated contact firing in a belt furnace with a peak temperature of 725 °C to introduce hydrogen into the bulk. Eventually they received another HF and HNA etch to remove SiN_x:H (and emitter).

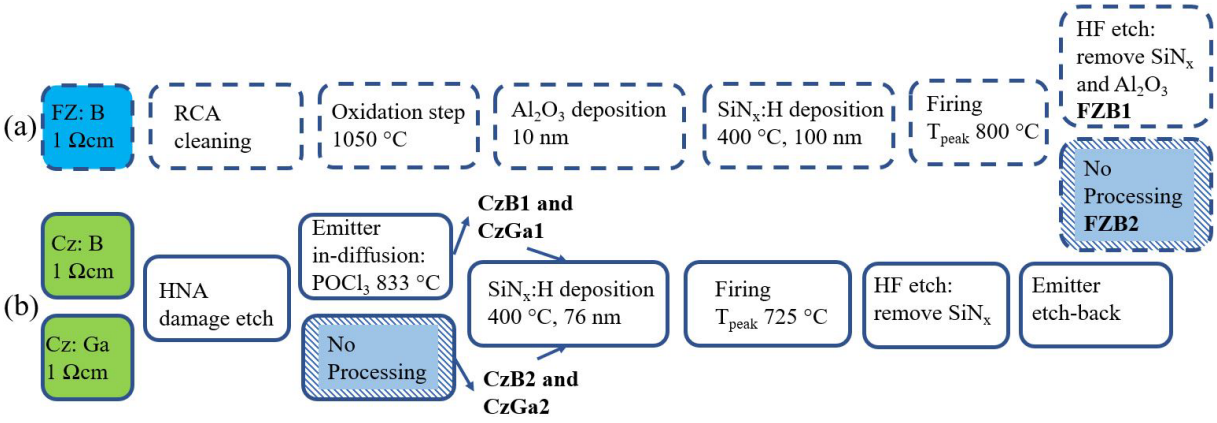

Figure 1. Processing steps for (a) FZ and (b) Cz wafers.

The wafers were cut in 10x10 mm^2 squares using a process laser and cleaved along the (110) plane.

2.2. Method: FT-IR Spectroscopy

To determine the concentration of hydrogen species in the wafers, FT-IR spectroscopy measurements were performed on a stack of the samples with pathlength d=1 cm (see Fig.2) with a Bruker IFS 125HR spectrometer under cryogenic temperatures (5 K). It is equipped with a globar light source, a KBr beam splitter, and a liquid-nitrogen-cooled InSb detector. Increased temperatures were controlled with a LakeShore 332. The calibration factors A for the different LVMs used to determine the concentrations are listed in Table 1.

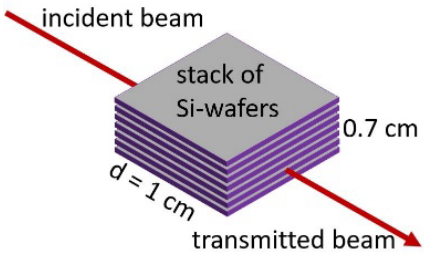

Figure 2. Schematic of the sample stack for FT-IR spectroscopical measurements.

Table 1. Calibration factors A and measured wavenumbers $\bar{\nu}$ for different LVMs.

LVM	A (cm^{-1})	$\bar{\nu}$ (cm^{-1})	Ref
H-B	$3.0 \cdot 10^{15}$	1904	[15]
H-Ga	$8.2 \cdot 10^{14}$	2173	[16]
O_i-H_2	$1.8 \cdot 10^{17}$	3731.0	[17]
H_2	$8.0 \cdot 10^{17}$	3618.4	[18]

3. Results and Discussion

3.1. FZ wafers: With and Without SiN_x:H Layer Present

Fig. 3 shows the subtracted transmittance spectra of an FZB1 and FZB2 sample, where the data with SiN_x:H (FZB2) were subtracted from the data without SiN_x:H (FZB1). We could not find the typical Si-H or N-H signals, expected at around 2160 cm^{-1} and 3350 cm^{-1} [13] for SiN_x:H layers. The absence of the signals indicates that the SiN_x:H does not interfere with the FT-IR measurement of the Si bulk in the chosen configuration.

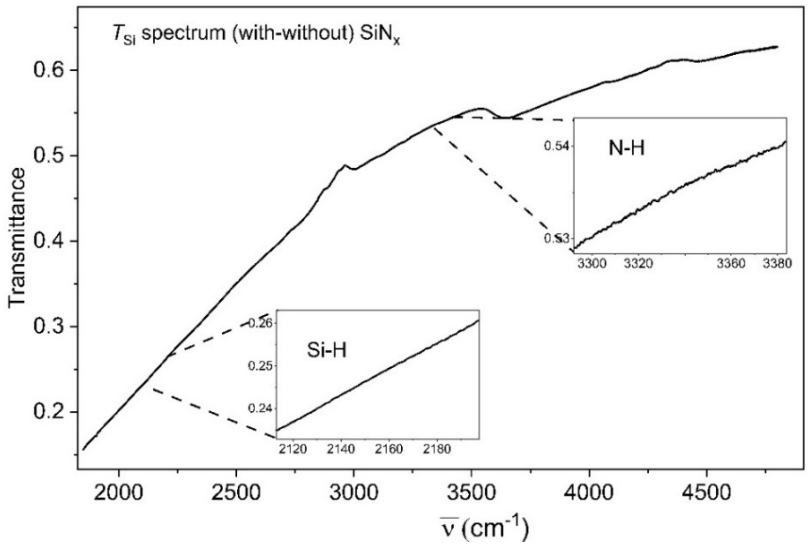

Figure 3. Subtracted transmission spectrum FZB2 – FZB1.

Fig. 4 shows the absorption spectra of two different FZ wafers. For each wafer one half retained the SiN_x:H layer as reference, denoted with FZB2, from the other half the layer was removed, denoted with FZB1. It is important to note, that for one wafer FZB1 is the upper half, while for the other wafer FZB1 is the lower half. Thus, for the two samples FZB1 and FZB2 were at different positions in the furnace during firing.

The resulting concentrations with uncertainties of H-B and H_2 species are given in Fig 4. in brackets.

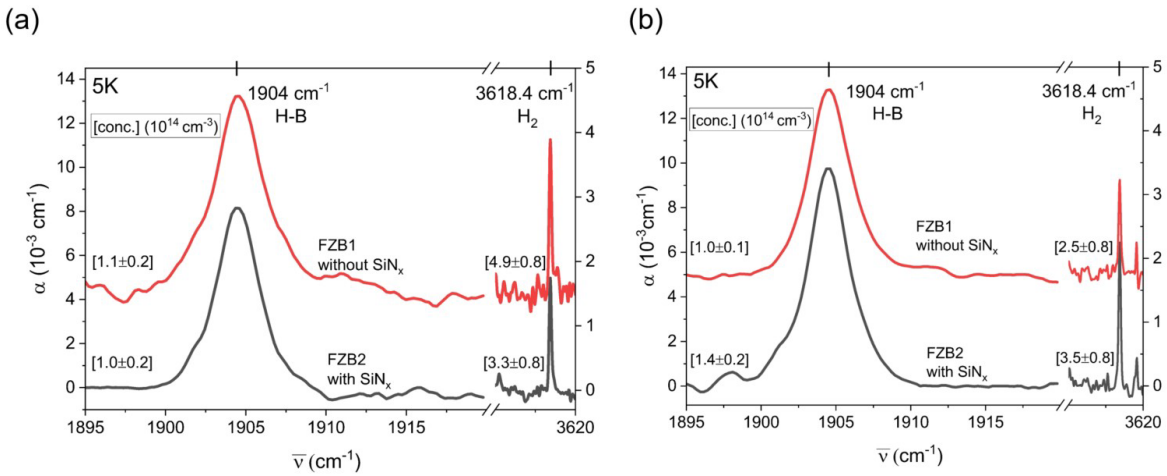

Figure 4. Absorption spectra (top) without and (bottom) with SiNx:H for two different wafers (a) and (b).

Considering the uncertainty of the results, the differences in concentration are not significant for each sample comparing FZB1 and FZB2. The measured H-B concentrations differ only within their uncertainties of ~$0.2 \cdot 10^{14}$ cm^{-3}. A larger deviation is seen in the H_2 concentration, which is found to be lower in (a) and higher in (b) for the FZB2 samples. Although the differences can be attributed to the spatial position of the wafer during firing and the existing temperature gradient within the furnace, one can also notice a larger uncertainty of $0.8 \cdot 10^{14}$ cm^{-3} for H_2 than for H-B concentrations.

3.2. Temperature Dependence of Absorption Spectra

We performed the measurements for FZB2 sample from the previous section at 35 K, 77 K (liquid N_2), 150 K, and 295 K. Fig. 5 shows the resulting (a) H-B and (b) H_2 spectra of the sample from Fig. 4 (b).

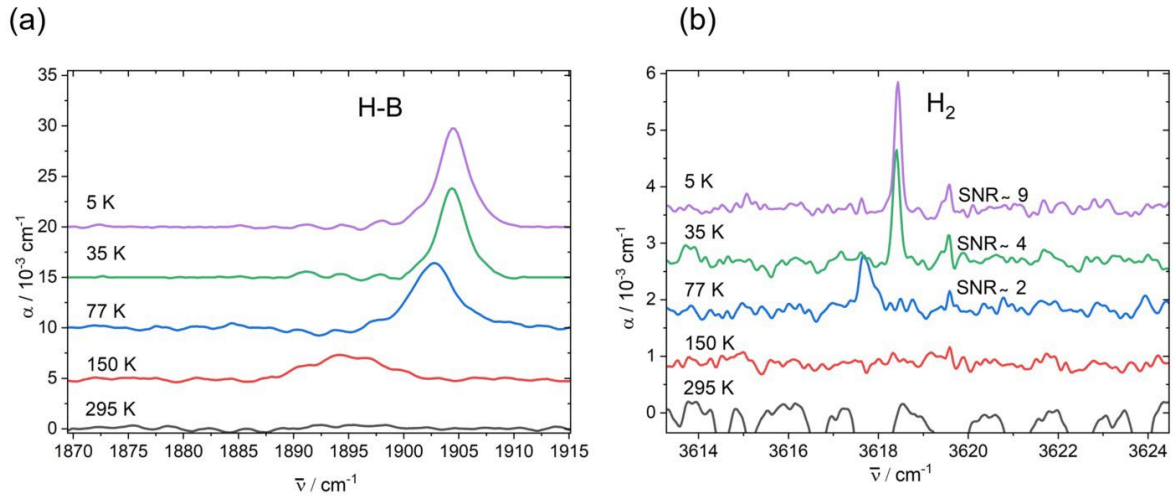

Figure 5. Absorption spectra for (a) H-B and (b) H_2 for different temperatures.

Both peaks shift to lower wavenumbers and broaden with increasing temperature. The shift originates from the decreased restoring force of the oscillating mode through thermal expansion. The broadening arises from a decreased lifetime of the LVM with increased temperature. The signal to noise ratio (SNR in Fig. 5 (b)) of H_2 decreases from SNR~9 at 5 K to SNR~2 at 77 K. While H-B exceeds the noise level until 150 K, 77 K are necessary for H_2. At room temperature (295 K) both signals stay below the noise level. The results of Fig. 5 show that the calibration factors vary with temperature and are presented in Table 2.

Table 2. Calibration factors *A* for H-B and H_2 of the sample shown in Fig. 5 for different temperatures.

***T* (K)**	***A* for H-B (cm^{-1})**	***A* for H_2 (cm^{-1})**
5	$3.0 \cdot 10^{15}$	$8.0 \cdot 10^{17}$
35	$(3.5 \pm 0.7) \cdot 10^{15}$	$(10 \pm 3) \cdot 10^{17}$
77	$(3.5 \pm 0.7) \cdot 10^{15}$	$(7 \pm 3) \cdot 10^{17}$
150	$(7.0 \pm 1.4) \cdot 10^{15}$	n.a.
295	n.a.	n.a.

The investigated temperatures from 5 K up to 77 K provide a precise evaluation of the peak area with detection limit of ~10^{13} cm^{-3}. In our study the H_2 peak disappeared at 150 K and denotes an increase that is probably closer to the room temperature limit of ~10^{14} cm^{-3} [14]. Because of the significant decrease in area of the H-B peak at 150 K we apply the same limit

here. Thus, liquid nitrogen as cooling medium is sufficient to detect both, H-B and H_2. However, through the increased SNR and broadened peaks the uncertainty of the evaluated areas increase compared to 5 K.

3.3. The Effect of Emitter Presence during Firing

Fig. 6 (a) and (b) show the absorption spectra for B- and Ga-doped Cz wafers. For both acceptor species, one wafer had a two-sided phosphorus emitter present during the firing process (CzB1 and CzGa1) with a subsequent etch-back (see Fig. 1). A second wafer set (CzB2 and CzGa2) had no emitter present during the same process.

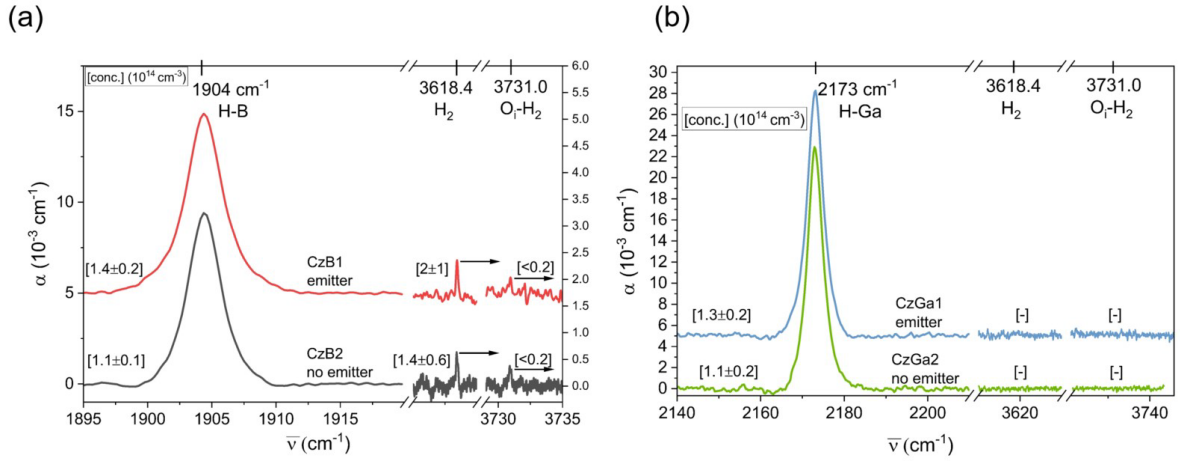

Figure 6. Absorption spectrum of (a) B- and (b) Ga-doped Si wafer with and without emitter. In (a) both peaks O_i-H_2, and H_2 are described by the right axis.

Slightly higher H-acceptor concentrations (see value in brackets in (a) for H-B peak and in (b) for H-Ga peak) are measured where the emitter was present during firing (CzB1 and CzGa1). As the differences are still within the uncertainties, it is difficult to draw conclusions on whether the emitter enhances hydrogen in-diffusion, but our results suggest a non-significant increase in H-species. Up to now we could not confirm Fischer's suspicion of increased H in the bulk due to a presence of an emitter during firing [19]. Instead, we propose the emitter acts as hydrogen reservoir in the initial state that releases hydrogen into the bulk during dark annealing. To gain a more comprehensive understanding, it may be beneficial to conduct additional research by subjecting the samples to dark annealing, which would increase the concentrations of H-B [12] and H-Ga [20].

An interesting difference between the two doping types is seen for the hydrogen molecule H_2. In the B-doped samples (Fig.6 (a)) a clear peak is visible over the noise level for H_2. At the same wavenumber the concentration does not exceed the noise level in the Ga-doped samples (Fig.6 (b)). Similarly, the O_i-H_2 peak is only apparent in the CzB samples. As H_2 molecule concentration seems to be closely connected to LeTID [12] our results can be a fruitful starting point for further investigations on observed differences between LeTID in B- and Ga-doped silicon.

4. Conclusion

Our study shows that the SiN_x:H layer does not affect the FT-IR measurements of wafer stacks. This finding simplifies the sample processing, as the SiN_x:H layer can be left intact without affecting the results. Additionally, it is found that the presence of an emitter during firing does not lead to a significant increase in hydrogen concentration in the Si bulk. However, further

experiments are necessary to investigate an increased H concentration as reason for the reported increased LeTID extend in Si.

Furthermore, this study reveals that B-doped and Ga-doped samples have similar initial concentrations of H-B and H-Ga respectively after identical processing. However, there is a significant difference in the spectra regarding the H_2 peaks. While both, H_2 and O_i-H_2 peaks are quantifiable in B-doped samples, the corresponding peaks do not exceed the noise level in Ga-doped samples.

While measurements at higher temperatures (liquid N_2) may result in some loss of accuracy, they offer the possibility of studying the material properties of B-doped Si wafers under simplified circumstances. We have determined varying calibration factors *A* for different temperatures to determine the concentration of H-B and H_2 in Si.

Data availability statement

The data that support the finding of this study are available from the corresponding author upon reasonable request.

Author contributions

N. Aßmann: conceptualization; data curation, formal analysis; investigation; project administration; visualization; writing – original draft; writing – review and editing. **R. Søndenå:** resources; validation; writing – review and editing. **B. Hammann:** resources; validation; writing – review and editing. **W. Kwapil:** resources; validation; writing – review and editing. **E. Monakhov:** conceptualization; funding acquisition; project administration; supervision; validation; writing – review and editing.

Competing interests

The authors declare no competing interests.

Funding

Funding for this work was provided by the Norwegian Research Council through the Research Center for Sustainable Solar Cell Technology (FME SUSOLTECH, No. 257639), as well as by the German Federal Ministry for Economic Affairs and Climate Action (No. 03EE1052B and 03EE152D).

Acknowledgement

The Research Council of Norway is acknowledged for the support to UiO MiNaLab as part of the Norwegian Micro- and Nanofabrication Facility, NorFab, project number 295864.

References

1. F. Chen, et al., Relationship between PECVD silicon nitride film composition and surface and edge passivation, European Photovoltaic Solar Energy Conference 2007, Sep 3-7, 2007, Milan, Italy.
2. B. Hallam, B. Tjahjono, and S. R. Wenham, “Effect of PECVD silicon oxynitride film composition on the surface passivation of silicon wafers,” Sol. Energy Mater Sol. Cells, vol. 96, pp. 173-179, Jan 2012, doi: 10.1016/J.SOLMAT.2011.09.052.

3. S. Wilking, A. Herguth, and G. Hahn, “Influence of hydrogenated passivation layers on the regeneration of boron-oxygen related defects,” Energy Procedia, vol. 38, pp. 642-648, 2013, doi: 10.1016/j.egypro.2013.07.328.
4. T. Niewelt et al., „Understanding the light-induced degradation at elevated temperatures: Similarities between multicrystalline and floatzone p-type silicon,” Prog. Photovolt., vol. 26, no. 8, pp. 533-542, 2018, doi: https://doi.org/10.1002/pip.2954.
5. R. Sharma et al., Hydrogen diffusion from PECVD silicon nitride into multicrystalline silicon wafers: Elastic recoil detection analysis (ERDA) measurements and impact on light and elevated temperature induced degradation (LeTID), SiliconPV 2019, April 8-10, 2019, Leuven, Belgium, doi: https://doi.org/10.1063/1.5123896.
6. D. Chen et al., “Progress in the understanding of light- and elevated temperature-induced degradation in silicon solar cells: A review,” Prog. Photovolt., vol. 29, no. 11, pp. 1180-1201, 2021, doi: https://doi.org/10.1002/pip.3362.
7. K. Ramspeck et al., Light Induced Degradation of Rear Passivated mc-Si Solar Cells, 27th EUPVSEC WIP, Sep 24-28, 2012, Frankfurt, Germany, doi: 10.4229/27thEUPVSEC2012-2DO.3.4
8. D. Chen et al., “Hydrogen induced degradation: A possible mechanism for light- and elevated temperature- induced degradation in n-type silicon,” Sol. Energy Mater Sol. Cells, vol. 185, pp. 174-182, 2018, https://doi.org/10.1016/j.solmat.2018.05.034.
9. F. Wolny et al., Wafer FT-IR – measuring interstitial oxygen on as cut and processed silicon wafers, SiliconPV 2016, March 07-09, 2016, Chambéry, France, doi: https://doi.org/10.1016/j.egypro.2016.07.076.
10. P. M. Weiser et al., “Hydrogen-related defects measured by infrared spectroscopy in multicrystalline silicon wafers throughout an illuminated annealing process,” J. Appl. Phys., vol. 127, no. 6, pp. 65703, 2020, doi: 10.1063/1.5142476.
11. R. Søndenå, P. M. Weiser, and E. Monakhov, Direct and indirect determination of hydrogen-boron complexes in float-zone silicon wafers, SiliconPV 2021, April 19-23, 2021, Hamelin, Germany, doi: https://doi.org/10.1063/5.0089274.
12. B. Hammann et al., “The Impact of Different Hydrogen Configurations on Light- and Elevated-Temperature- Induced Degradation,” IEEE J. Photovolt., vol. 13, no. 2, pp. 224-235, 2023, doi: 10.1109/JPHOTOV.2023.3236185.
13. I. Jonak-Auer, R. Meisels, and F. Kuchar, „Determination of the hydrogen concentration of silicon nitride layers by Fourier transform infrared spectroscopy,” Infrared Phys Technol, vol. 38, no. 4, pp. 223-226, 1997, doi: https://doi.org/10.1016/S1350-4495(97)00011-X.
14. J. Simon, A. Herguth, and G. Hahn, “Quantitative analysis of boron–hydrogen pair dynamics by infrared absorption measurements at room temperature,” J. Appl. Phys., vol. 131, no. 23, pp. 135703, 2022, doi: https://doi.org/10.1063/5.0090965.
15. S. A. McQuaid et al., “Concentration of atomic hydrogen diffused into silicon in the temperature range 900–1300 °C,” Appl. Phys Lett., vol. 58, no. 25, pp. 2933-2935, 1991, doi: https://doi.org/10.1063/1.104726.
16. M. Stavola et al., “Vibrational characteristics of acceptor-hydrogen complexes in silicon,” Appl. Phys Lett., vol. 50, no. 16, pp. 1086-1088, 1987, doi: https://doi.org/10.1063/1.97978.
17. R. E. Pritchard et al., “Interactions of hydrogen molecules with bond-centered interstitial oxygen and another defect center in silicon,” Phys. Rev. B, vol 56, no. 20, pp. 13778-13125, Nov 1997, doi: 10.1103/PhysRevB.56.13118.
18. R. E. Pritchard et al., “Hydrogen molecules in boron-doped crystalline silicon,” Semicond. Sci. Technol., vol 14, no. 1, pp. 77, Jan 1999, doi: 10.1088/0268-1242/14/1/011.
19. C. Fischer et al., “Influence of highly doped layers on hydrogen in-diffusion into crystalline silicon,” Sol. Energy Mater Sol. Cells, vol. 250, pp. 112056, 2023, doi: https://doi.org/10.1016/j.solmat.2022.112056.
20. Y. Acker, J. Simon, and A. Herguth, “Formation Dynamics of BH and GaH-Pairs in Crystalline Silicon During Dark Annealing,” Phys. Status Solidi A, vol. 219, no. 17, pp. 2200142, 2022, doi: https://doi.org/10.1002/pssa.202200142.